

# Boundary-Value Problem for Electromagnetic Fields in Cylindrical Conductor with Circumferential Electrodes Excited by AC-Current

H. E. Wilhelm \*, S. H. Hong \*\*, and D. A. Boonzaier

Department of Bioengineering and Groote Schuur Hospital, University of Cape Town, Cape Town, Republic of South Africa

Z. Naturforsch. **33a**, 1161–1168 (1978); received June 12, 1978

The boundary-value problem for the electromagnetic fields  $\mathbf{E}(\mathbf{r}, t) = \{E_r(r, z, t), 0, E_z(r, z, t)\}$  and  $\mathbf{B}(\mathbf{r}, t) = \{0, B_\theta(r, z, t), 0\}$  in an electrically conducting cylinder of radius  $r = a$  and infinite length ( $-\infty \leq z \leq +\infty$ ) is treated, which are excited by a periodic ac-current  $I(t) = I_0 \cos \omega t$  entering and leaving the cylinder through circumferential electrodes at  $r = a$  and  $z = \pm c$ . Solutions for  $\mathbf{E}(\mathbf{r}, t)$  and  $\mathbf{B}(\mathbf{r}, t)$  are obtained in terms of Fourier integrals which are reduced to infinite series by means of the residue theorem. Graphical presentations of the fields  $\mathbf{E}(\mathbf{r}, z, t)$  and  $\mathbf{B}(\mathbf{r}, z, t)$  versus  $z$  and  $r$  for times  $\omega t = 0$  and  $\pi/2$  are given which show the relative amplitude and phase relations of the fields. An application of the results to medical physics is discussed concerning the measurement of the electrical conductivity of the tissue of limbs.

## Introduction

In a classical investigation, Sommerfeld evaluated the electromagnetic field of an infinitely long wire carrying a periodic electric current [1]. We treat a similar, though more complex boundary-value problem for the electromagnetic field in a cylindrical conductor of infinite length  $L = \infty$ , which is supplied with a periodic current  $I(t) = I_0 \cos \omega t$  through circumferential electrodes located on the surface  $r = a$  of the conductor at the axial positions  $z = \pm c$  (Figure 1). For the case of electrodes of non-vanishing width,  $|\Delta z| > 0$ , and quasi-infinite conductivity, the electric potential within the electrode contact surface and the radial potential gradient within the remaining surface of the conductor are given as boundary conditions. Mixed boundary-value problems of this type lead to dual integral equations which cannot, in general, be solved in closed form [2]. This is probably the reason why the fundamental electromagnetic boundary-value problem under consideration has not been solved in the literature.

Under the assumption that the axial width  $\Delta z$  of the electrodes is small compared with all characteristic dimensions of the system,  $|\Delta z| \ll a < \infty$  and

Reprint requests to Prof. Dr. H. E. Wilhelm, Dept. of Electrical Engineering, Colorado State University, Fort Collins, CO 80523, U.S.A.

\* On sabbatical leave from the Department of Electrical Engineering, Colorado State University, Fort Collins, Colorado.

\*\* Department of Electrical Engineering, Colorado State University, Fort Collins, Colorado.

$|\Delta z| \ll L = \infty$ , the injected current distributions at the electrode surfaces can be represent as Dirac functions. This approximation permits us to reduce the mixed boundary-value problem to a Dirichlet problem. It is remarkable that the mixed boundary

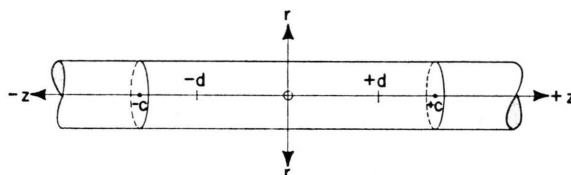


Fig. 1. Geometry of conducting cylinder of radius  $r = a$  with circumferential electrodes at  $r = a$ ,  $z = \pm c$ .

conditions for electrodes of nonvanishing width  $|\Delta z| > 0$  could be taken into account rigorously by means of a continuous superposition of Dirac functions at axial positions  $z$  within the electrode surface. This approach would represent an alternative to the solution of mixed boundary-value problems based on distribution theory.

This electromagnetic boundary-value problem arose in connection with the evaluation of the zero-order response of a cylindrical model for a limb ( $\sigma \cong 10^{-1} \text{ mho m}^{-1}$ ) subject to an ac-current via ring electrodes of frequency  $\nu = 10^5 \text{ sec}^{-1}$  and intensity  $I_0 = 10^{-3} \text{ amps}$ . The resulting potential difference observed at the surface  $r = a$  of the limb allows determination of the impedance of the limb at the frequency  $\nu$ . The (weak) conductivity pulses caused by the pulsating blood flow give rise to a small perturbation of the electric potential from which the speed of the blood flow can be determined [3, 4].



Dieses Werk wurde im Jahr 2013 vom Verlag Zeitschrift für Naturforschung in Zusammenarbeit mit der Max-Planck-Gesellschaft zur Förderung der Wissenschaften e.V. digitalisiert und unter folgender Lizenz veröffentlicht: Creative Commons Namensnennung-Keine Bearbeitung 3.0 Deutschland Lizenz.

Zum 01.01.2015 ist eine Anpassung der Lizenzbedingungen (Entfall der Creative Commons Lizenzbedingung „Keine Bearbeitung“) beabsichtigt, um eine Nachnutzung auch im Rahmen zukünftiger wissenschaftlicher Nutzungsformen zu ermöglichen.

This work has been digitalized and published in 2013 by Verlag Zeitschrift für Naturforschung in cooperation with the Max Planck Society for the Advancement of Science under a Creative Commons Attribution-NoDerivs 3.0 Germany License.

On 01.01.2015 it is planned to change the License Conditions (the removal of the Creative Commons License condition “no derivative works”). This is to allow reuse in the area of future scientific usage.

### Boundary-Value Problem

In general, the electromagnetic fields  $\mathbf{E}(\mathbf{r}, t)$  and  $\mathbf{B}(\mathbf{r}, t)$  produced by a current density  $\mathbf{j}(\mathbf{r}, t)$  are determined by Maxwell's equations with displacement current  $\delta = \mu \varepsilon \partial \mathbf{E} / \partial t$  ( $\mu, \varepsilon =$  magnetic and electrical permeability). The electromagnetic field propagates approximately with the speed of light  $u_0 = 1/\mu \varepsilon \cong 3 \times 10^8 \text{ m sec}^{-1}$  along the conductor [1]. Accordingly, if the frequency  $\omega$  of the periodic current source is small compared to

$$u_0/\lambda, \lambda \sim \max(a, c),$$

the electromagnetic field can be assumed to adjust itself quasi-instantaneously to the relatively slow changes of  $\mathbf{j}(\mathbf{r}, t)$ . In this situation, the theory of quasi-stationary currents is applicable, i.e. Maxwell's equations without displacement current [5]:

$$\nabla \times \mathbf{E} = -\partial \mathbf{B} / \partial t, \quad \nabla \cdot \mathbf{E} = 0, \quad (1)$$

$$\nabla \times \mathbf{B} = \mu \mathbf{j}, \quad \nabla \cdot \mathbf{B} = 0, \quad (2)$$

where

$$\mathbf{j} = \sigma \mathbf{E} \quad (3)$$

is Ohm's law for an isotropic conductor of relaxation time  $\tau_c \ll \omega^{-1}$  in a frame of reference in which the conductor is at rest. For example, for

$$\lambda \sim c = 1 \text{ m} > a \quad \text{and} \quad \omega = 2\pi \times 10^5 \text{ sec}^{-1},$$

the condition for neglecting the displacement current is well satisfied,

$$\begin{aligned} \omega \lambda &\sim 2\pi \times 10^5 \text{ m sec}^{-1} \ll u_0 \\ &\cong 3 \times 10^8 \text{ m sec}^{-1}. \end{aligned}$$

The system under consideration is a cylindrical conductor of radius  $a$ , length  $L = \infty$ , and homogeneous conductivity  $\sigma$ . An ac-current

$$I(t) = I_0 \cos \omega t = I_0 \operatorname{Re} \exp \{i \omega t\} \quad (4)$$

is injected through the central segment  $2c$  of this conductor by means of ring electrodes at  $r = a$  and  $z = \pm c$ , which are assumed to be of vanishing width (Figure 1). The injected current density entering the surface of the cylinder is, therefore, radial and given by

$$\begin{aligned} j_r(r = a, z, t) &= -\mu^{-1} \partial B_\theta(r = a, z, t) / \partial z \\ &= (I_0 / 2\pi a) \cos \omega t [\delta(z + c) - \delta(z - c)]. \end{aligned} \quad (5)$$

The electromagnetic field in the conductor is of the form

$$\begin{aligned} \mathbf{B}(\mathbf{r}, t) &= \{0, B_\theta(r, z, t), 0\}, \\ \mathbf{E}(\mathbf{r}, t) &= \{E_r(r, z, t), 0, E_z(r, z, t)\} \end{aligned} \quad (6)$$

where

$$\mathbf{E} = D \{-\partial B_\theta / \partial z, 0, r^{-1} \partial(r B_\theta) / \partial r\} \quad (7)$$

by Eqs. (2)–(3), and  $D$  is the diffusion coefficient of the electromagnetic field,

$$D = 1/\mu \sigma [\text{m}^2 \text{ sec}^{-1}]. \quad (8)$$

In accordance with Eqs. (1)–(8), the complex dimensionless version  $\mathcal{B}(\varrho, \zeta, \tau)$  of the azimuthal magnetic field  $B_\theta(r, z, t)$  is described by the complex, parabolic boundary-value problem:

$$\frac{\partial \mathcal{B}}{\partial \tau} = \frac{\partial^2 \mathcal{B}}{\partial \varrho^2} + \frac{1}{\varrho} \frac{\partial \mathcal{B}}{\partial \varrho} - \frac{\mathcal{B}}{\varrho^2} + \frac{\partial^2 \mathcal{B}}{\partial \zeta^2}, \quad (9)$$

$$\begin{aligned} & -[\partial \mathcal{B}(\varrho, \zeta, \tau) / \partial \zeta]_{\zeta=\bar{\zeta}} \\ & = e^{i\tau} [\delta(\zeta + \bar{c}) - \delta(\zeta - \bar{c})], \quad |\zeta| \leq \infty, \end{aligned} \quad (10)$$

$$\partial[\varrho \mathcal{B}(\varrho, \zeta, \tau)] / \partial \varrho \rightarrow 0, \quad |\zeta| \rightarrow \infty, \quad (11)$$

where

$$\begin{aligned} \varrho &= r/(D/\omega)^{1/2}, \quad 0 \leq \varrho \leq \bar{a}, \\ \bar{a} &= a/(D/\omega)^{1/2}, \end{aligned} \quad (12)$$

$$\begin{aligned} \zeta &= z/(D/\omega)^{1/2}, \quad -\infty \leq \zeta \leq +\infty, \\ \bar{c} &= c/(D/\omega)^{1/2}, \end{aligned} \quad (13)$$

$$\tau = \omega t, \quad 0 \leq \tau \leq \infty, \quad (14)$$

and

$$\begin{aligned} \operatorname{Re} \mathcal{B}(\varrho, \zeta, \tau) &= B_\theta(r, z, t) / B_0, \\ B_0 &\equiv \mu I_0 / 2\pi a. \end{aligned} \quad (15)$$

Equation (9) represents the diffusion equation for the magnetic field in the quasi-stationary approximation [5]. Equation (10) is the boundary condition corresponding to Equation (5). Equation (11) is an improper boundary condition considering that the axial current density vanishes at infinity,

$$\begin{aligned} j_z(r, z, t) &= \mu^{-1} \partial[r B_\theta(r, z, t)] / r \partial r \rightarrow 0, \\ |z| &\rightarrow \infty. \end{aligned}$$

By Eqs. (2)–(3), the electric field components are obtained from the solution for  $\mathcal{B}(\varrho, \zeta, \tau)$  as

$$\begin{aligned} E_r(r, z, t) &= -E_0 \operatorname{Re} \{\partial \mathcal{B}(\varrho, \zeta, \tau) / \partial \zeta\}, \\ E_z(r, z, t) &= +E_0 \operatorname{Re} \{\partial[\varrho \mathcal{B}(\varrho, \zeta, \tau)] / \partial \varrho\}, \\ E_0 &\equiv (D\omega)^{1/2} \mu I_0 / 2\pi a. \end{aligned} \quad (16)$$

### Analytical Solution

The partial solutions of the boundary-value problem in Eqs. (9)–(11) are oscillations at the dimen-

sionless frequency  $\bar{\omega} = 1$ , and are of the form

$$\mathcal{B}_\alpha(\rho, \zeta, \tau) \propto I_1(\sqrt{i + \alpha^2} \rho) \cos \alpha \zeta \exp(i\tau),$$

since  $\partial \mathcal{B}(\rho, \zeta, \tau) / \partial \zeta$  is asymmetric with respect to the plane  $\zeta = 0$  by Equation (10). Accordingly, the general solution of Eqs. (9)–(11) should be representable by the Fourier integral over the continuous eigenvalues  $\alpha$  ( $|\zeta| \leq \infty$ ),

$$\mathcal{B}(\rho, \zeta, \tau) = e^{i\tau} \int_0^\infty A(\alpha) I_1(\sqrt{i + \alpha^2} \rho) \cos \alpha \zeta d\alpha \quad (17)$$

where

$$\begin{aligned} \int_0^\infty A(\alpha) \alpha I_1(\sqrt{i + \alpha^2} \bar{a}) \sin \alpha \zeta d\alpha \\ = - (2/\pi) \int_0^\infty \sin \alpha \bar{c} \sin \alpha \zeta d\alpha \end{aligned} \quad (18)$$

by the boundary condition (10). In Eq. (18) the Dirac functions  $\delta(\zeta \pm \bar{c})$  of Eq. (10) have been expanded as Fourier integrals,

$$\begin{aligned} \delta(\zeta + \bar{c}) - \delta(\zeta - \bar{c}) \\ = - (2/\pi) \int_0^\infty \sin \alpha \bar{c} \sin \alpha \zeta d\alpha. \end{aligned} \quad (19)$$

Application of the inverse Hankel transform to Eq. (18) gives for the Fourier amplitudes

$$A(\alpha) = - \frac{2}{\pi} \frac{\sin \alpha \bar{c}}{\alpha} I_1^{-1}(\sqrt{i + \alpha^2} \bar{a}). \quad (20)$$

Combining of Eqs. (17) and (20) yields the general solution for the magnetic field in complex, dimensionless representation:

$$\begin{aligned} \mathcal{B}(\rho, \zeta, \tau) = \\ - \frac{2}{\pi} e^{i\tau} \int_0^\infty \frac{\sin \alpha \bar{c}}{\alpha} \frac{I_1(\sqrt{i + \alpha^2} \rho)}{I_1(\sqrt{i + \alpha^2} \bar{a})} \cos \alpha \zeta d\alpha. \end{aligned} \quad (21)$$

As will be shown, this solution satisfies also the improper boundary condition (11). By means of Eq. (16), one derives from Eq. (21) the complex, dimensionless solutions for the electric field:

$$\begin{aligned} \mathcal{E}_\rho(\rho, \zeta, \tau) = \\ - \frac{2}{\pi} e^{i\tau} \int_0^\infty \sin \alpha \bar{c} \frac{I_1(\sqrt{i + \alpha^2} \rho)}{I_1(\sqrt{i + \alpha^2} \bar{a})} \sin \alpha \zeta d\alpha, \end{aligned} \quad (22)$$

$$\begin{aligned} \mathcal{E}_\zeta(\rho, \zeta, \tau) = \\ - \frac{2}{\pi} e^{i\tau} \int_0^\infty \sqrt{i + \alpha^2} \frac{\sin \alpha \bar{c}}{\alpha} \frac{I_0(\sqrt{i + \alpha^2} \rho)}{I_1(\sqrt{i + \alpha^2} \bar{a})} \cos \alpha \zeta d\alpha. \end{aligned} \quad (23)$$

The integrands in Eqs. (21)–(23) are even in  $\alpha$ , so that the Fourier integral solutions can be rewritten, in the complex  $\alpha$ -plane, as ( $\text{sgn}(x) = \pm 1$ ,  $x \gtrless 0$ ;  $\text{sgn}(x) = 0$ ,  $x = 0$ ):

$$\begin{aligned} \mathcal{B}(\rho, \zeta, \tau) = \frac{i e^{i\tau}}{2\pi} \int_{-\infty}^{+\infty} [\text{sgn}(\bar{c} + \zeta) e^{i\alpha|\bar{c} + \zeta|} \\ + \text{sgn}(\bar{c} - \zeta) e^{i\alpha|\bar{c} - \zeta|}] \frac{I_1(\sqrt{i + \alpha^2} \rho)}{I_1(\sqrt{i + \alpha^2} \bar{a})} \frac{d\alpha}{\alpha}, \end{aligned} \quad (24)$$

$$\begin{aligned} \mathcal{E}_\rho(\rho, \zeta, \tau) = \frac{e^{i\tau}}{2\pi} \int_{-\infty}^{+\infty} (e^{i\alpha|\bar{c} + \zeta|} \\ - e^{i\alpha|\bar{c} - \zeta|}) \frac{I_1(\sqrt{i + \alpha^2} \rho)}{I_1(\sqrt{i + \alpha^2} \bar{a})} d\alpha, \end{aligned} \quad (25)$$

$$\begin{aligned} \mathcal{E}_\zeta(\rho, \zeta, \tau) = \frac{i e^{i\tau}}{2\pi} \int_{-\infty}^{+\infty} \sqrt{i + \alpha^2} [\text{sgn}(\bar{c} + \zeta) e^{i\alpha|\bar{c} + \zeta|} \\ + \text{sgn}(\bar{c} - \zeta) e^{i\alpha|\bar{c} - \zeta|}] \frac{I_0(\sqrt{i + \alpha^2} \rho)}{I_1(\sqrt{i + \alpha^2} \bar{a})} \frac{d\alpha}{\alpha}. \end{aligned} \quad (26)$$

Comparison of Eqs. (24) and (26) with Eqs. (21) and (23) respectively indicates that poles have been generated at  $\alpha = 0$  by replacing the trigonometric functions by complex exponential functions. The path of integration for the integrals in Eqs. (24) and (26) has to be intended through a semi-circle  $C_{\mathcal{R}_0}$  because of the pole at  $\alpha = 0$  (Fig. 2a), whereas the closed contour for the integral in Eq. (25) is a straight line along the real axis closed by the semi-circle  $\mathcal{R}_\infty$  (Figure 2b). The contribution to the in-

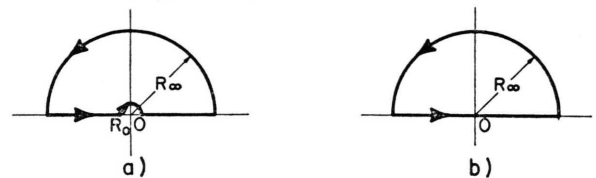


Fig. 2. Paths of integration a) and b) in the complex plane.

tegrals from the pole at  $\alpha = 0$  is  $-\pi i \text{Res}(\alpha = 0)$  in the limit  $\mathcal{R}_0 \rightarrow 0$ , the negative sign being due to the negative sense of the semi-circle  $C_{\mathcal{R}_0}$ . The integral along the semi-circle  $\mathcal{R}_\infty$  in Eq. (24) tends to zero in the limit  $\mathcal{R}_\infty \rightarrow 0$  by Jordan's lemma. The zeros of the modified Bessel function of order one in the denominator of Eqs. (24)–(26) produce poles in the upper half-plane at

$$\begin{aligned} \alpha = + i \sqrt{i + \alpha_p^2} \equiv u_p + i v_p, \\ v = 1, 2, 3, \dots, \end{aligned} \quad (27)$$

where

$$\begin{aligned} u_p = - 2^{-1/2} [-\alpha_p^2 + (1 + \alpha_p^4)^{1/2}]^{1/2} \rightarrow 0, \\ \alpha_p \rightarrow \infty, \end{aligned} \quad (28)$$

$$v_p = +2^{-1/2}[-\alpha_p^2 + (1 + \alpha_p^4)^{1/2}]^{-1/2} \rightarrow \alpha_p, \\ \alpha_p \rightarrow \infty, \quad (29)$$

and

$$J_1(\alpha_p \bar{a}) = 0, \quad p = 1, 2, 3, \dots, \quad (30)$$

determines  $\alpha_p \bar{a} \geq 0$  as the roots of the ordinary Bessel function of order one. In accordance with the residue theorem, the Fourier integrals for the electromagnetic fields in Eqs. (24)–(26) reduce to sums over one half of the residue of the pole at  $\alpha = 0$  and the infinitely many residues of the poles at  $\alpha = i\sqrt{1 + \alpha_p^2}(\delta_{\rho\bar{a}} = 1; 0 \text{ for } \rho = \bar{a}; \neq \bar{a})$ :

$$\mathcal{B}(\rho, \zeta, \tau) = -\frac{1}{2} \frac{J_1(\rho e^{i3\pi/4})}{J_1(\bar{a} e^{i3\pi/4})} [\operatorname{sgn}(\bar{c} + \zeta) + \operatorname{sgn}(\bar{c} - \zeta)] e^{i\tau} \\ - \frac{1}{\bar{a}} \sum_{p=1}^{\infty} \frac{\alpha_p(\alpha_p^2 - i)}{1 + \alpha_p^4} \frac{J_1(\alpha_p \rho)}{J_0(\alpha_p \bar{a})} F_p(\zeta, \tau), \quad (31)$$

$$\mathcal{E}_\rho(\rho, \zeta, \tau) = -\delta_{\rho\bar{a}}[\delta(\zeta - \bar{c}) - \delta(\zeta + \bar{c})] e^{i\tau} \\ - \frac{1}{\bar{a}} \sum_{p=1}^{\infty} \frac{\alpha_p(p_p - i q_p)}{p_p^2 + q_p^2} \frac{J_1(\alpha_p \rho)}{J_0(\alpha_p \bar{a})} G_p(\zeta, \tau), \quad (32)$$

$$\mathcal{E}_\zeta(\rho, \zeta, \tau) = -\frac{1}{2} \frac{J_0(\rho e^{i3\pi/4})}{J_1(\bar{a} e^{i3\pi/4})} [\operatorname{sgn}(\bar{c} + \zeta) + \operatorname{sgn}(\bar{c} - \zeta)] e^{i(\tau + 3\pi/4)} \\ - \frac{1}{\bar{a}} \sum_{p=1}^{\infty} \frac{\alpha_p^2(\alpha_p^2 - i)}{1 + \alpha_p^4} \frac{J_0(\alpha_p \rho)}{J_0(\alpha_p \bar{a})} F_p(\zeta, \tau), \quad (33)$$

where

$$p_p = 2^{-1/2}[\alpha_p^2 + (1 + \alpha_p^4)^{1/2}]^{+1/2} \sim \alpha_p^{+1}, \\ \alpha_p \gg 1, \quad (34)$$

$$q_p = 2^{-1/2}[\alpha_p^2 + (1 + \alpha_p^4)^{1/2}]^{-1/2} \sim \alpha_p^{-1}, \\ \alpha_p \gg 1, \quad (35)$$

and

$$F_p(\zeta, \tau) = \operatorname{sgn}(\bar{c} + \zeta) \cdot \exp[-p_p|\bar{c} + \zeta| + i(\tau - q_p|\bar{c} + \zeta|)] \\ + \operatorname{sgn}(\bar{c} - \zeta) \exp[-p_p|\bar{c} - \zeta| + i(\tau - q_p|\bar{c} - \zeta|)], \quad (36)$$

$$G_p(\zeta, \tau) = \operatorname{sgn}^2(\bar{c} + \zeta) \cdot \exp[-p_p|\bar{c} + \zeta| + i(\tau - q_p|\bar{c} + \zeta|)] \\ - \operatorname{sgn}^2(\bar{c} - \zeta) \exp[-p_p|\bar{c} - \zeta| + i(\tau - q_p|\bar{c} - \zeta|)]. \quad (37)$$

Finally, by taking the real parts of the Eqs. (31) to (33), we find the dimensionless, real electromagnetic

fields inside the conductor,

$$0 \leq \rho \leq \bar{a}, \quad -\infty \leq \zeta \leq +\infty:$$

$$\operatorname{Re} \mathcal{B}(\rho, \zeta, \tau) = -[\operatorname{sgn}(\bar{c} + \zeta) + \operatorname{sgn}(\bar{c} - \zeta)] \quad (38)$$

$$\cdot h_1(\rho, \tau) - \frac{1}{\bar{a}} \sum_{p=1}^{\infty} \frac{\alpha_p}{1 + \alpha_p^4} \frac{J_1(\alpha_p \rho)}{J_0(\alpha_p \bar{a})} f_p(\zeta, \tau),$$

$$\operatorname{Re} \mathcal{E}_\rho(\rho, \zeta, \tau) = -\delta_{\rho\bar{a}}[\delta(\zeta - \bar{c}) - \delta(\zeta + \bar{c})] \quad (39)$$

$$\cdot \cos \tau - \frac{1}{\bar{a}} \sum_{p=1}^{\infty} \frac{\alpha_p}{p_p^2 + q_p^2} \frac{J_1(\alpha_p \rho)}{J_0(\alpha_p \bar{a})} g_p(\zeta, \tau),$$

$$\operatorname{Re} \mathcal{E}_\zeta(\rho, \zeta, \tau) = -[\operatorname{sgn}(\bar{c} + \zeta) + \operatorname{sgn}(\bar{c} - \zeta)] \quad (40)$$

$$\cdot h(\rho, \tau) - \frac{1}{\bar{a}} \sum_{p=1}^{\infty} \frac{\alpha_p^2}{1 + \alpha_p^4} \frac{J_0(\alpha_p \rho)}{J_0(\alpha_p \bar{a})} f_p(\zeta, \tau),$$

where

$$J_0(x e^{i3\pi/4}) = \operatorname{ber}(x) + i \operatorname{bei}(x), \\ J_1(x e^{i3\pi/4}) = \operatorname{ber}_1(x) + i \operatorname{bei}_1(x), \quad (41)$$

and

$$h_1(\rho, \tau) = 2^{-1}[\operatorname{ber}_1^2(\bar{a}) + \operatorname{bei}_1^2(\bar{a})]^{-1} \\ \cdot \{[\operatorname{ber}_1(\bar{a}) \cos \tau + \operatorname{bei}_1(\bar{a}) \sin \tau] \cdot \operatorname{ber}_1(\rho) + [\operatorname{bei}_1(\bar{a}) \cos \tau - \operatorname{ber}_1(\bar{a}) \sin \tau] \operatorname{bei}_1(\rho)\}, \quad (42)$$

$$h(\rho, \tau) = -2^{-3/2}[\operatorname{ber}_1^2(\bar{a}) + \operatorname{bei}_1^2(\bar{a})]^{-1} \\ \cdot \{[\operatorname{ber}_1(\bar{a}) \cos \tau + \operatorname{bei}_1(\bar{a}) \sin \tau] \cdot [\operatorname{ber}(\rho) + \operatorname{bei}(\rho)] \\ - [\operatorname{bei}_1(\bar{a}) \cos \tau - \operatorname{ber}_1(\bar{a}) \sin \tau] \cdot [\operatorname{ber}(\rho) - \operatorname{bei}(\rho)]\}, \quad (43)$$

$$f_p(\zeta, \tau) = \operatorname{sgn}(\bar{c} + \zeta) [\alpha_p^2 \cos(\tau - q_p|\bar{c} + \zeta|) + \sin(\tau - q_p|\bar{c} + \zeta|)] \\ \cdot \exp\{-p_p|\bar{c} + \zeta|\} + \operatorname{sgn}(\bar{c} - \zeta) \cdot [\alpha_p^2 \cos(\tau - q_p|\bar{c} - \zeta|) + \sin(\tau - q_p|\bar{c} - \zeta|)] \\ \cdot \exp\{-p_p|\bar{c} - \zeta|\}, \quad (44)$$

$$g_p(\zeta, \tau) = \operatorname{sgn}^2(\bar{c} + \zeta) [p_p \cos(\tau - q_p|\bar{c} + \zeta|) + q_p \sin(\tau - q_p|\bar{c} + \zeta|)] \\ \cdot \exp\{-p_p|\bar{c} + \zeta|\} - \operatorname{sgn}^2(\bar{c} - \zeta) \cdot [p_p \cos(\tau - q_p|\bar{c} - \zeta|) + q_p \sin(\tau - q_p|\bar{c} - \zeta|)] \\ \cdot \exp\{-p_p|\bar{c} - \zeta|\}. \quad (45)$$

It is seen that the azimuthal magnetic field [Eq. (38)] is symmetrical with respect to the central plan  $\zeta = 0$ , i.e.,

$$\mathcal{B}(\rho, -\zeta, \tau) = \mathcal{B}(\rho, +\zeta, \tau).$$

The radial electric field [Eq. (39)] is asymmetrical with respect to the central plane, i.e.,

$$\mathcal{E}_\rho(\rho, -\zeta, \tau) = -\mathcal{E}_\rho(\rho, +\zeta, \tau).$$

The axial electric field [Eq. (40)] is symmetrical with respect to the plane  $\zeta = 0$ , i.e.,

$$\mathcal{E}_\zeta(\rho, -\zeta, \tau) = \mathcal{E}_\zeta(\rho, +\zeta, \tau).$$

The electromagnetic field oscillates with the frequency  $\omega$  in time  $t$ , and any of the field components  $\mathcal{F}(\rho, \zeta, \tau)$  in Eqs. (38)–(40) has the period  $\Delta\tau = 2\pi$ ,

$$\mathcal{F}(\rho, \zeta, \tau + 2\pi n) = \mathcal{F}(\rho, \zeta, \tau), \quad (46)$$

$$n = 0, \pm 1, \pm 2, \dots$$

Furthermore, it is recognized that the electromagnetic field components in Eqs. (38)–(40) satisfy the improper boundary condition

$$\mathcal{F}(\rho, \zeta, \tau) \rightarrow 0, \quad |\zeta| \rightarrow \infty.$$

In Figs. 3, 4, and 5 the (azimuthal) magnetic field  $\mathcal{B}(\rho, \zeta, \tau)$ , the radial,  $\mathcal{E}_\rho(\rho, \zeta, \tau)$ , and axial,  $\mathcal{E}_\zeta(\rho, \zeta, \tau)$ , electric fields are represented versus  $-\infty \leq \zeta \leq +\infty$  at various radial distances  $0 < \rho < \bar{a}$  and times  $\tau = 0, \pi/2$ . The dimensionless parameters are taken as  $\bar{a} = 1$  and  $\bar{c} = 10$  so that the ratio of the dimensional geometry constants is  $c/a = 10$ . Sufficient accuracy of the field distributions was obtained by approximating the infinite series solutions by the first hundred terms on the computer,  $\nu = 1, 2, \dots, \nu_{\max} \equiv 10^2$ .

Figure 3 shows that  $\mathcal{B}(\rho, \zeta, \tau)$  exhibits a plateau in the axial region  $|\zeta| < \bar{c}$  for any  $\rho = \text{const} < \bar{a}$  and approaches a square step for  $\rho = \bar{a}$ , since there is no net current flow through the conductor cross section  $0 \leq \rho \leq \bar{a}$  for any  $|\zeta| \geq \bar{c}$ . Due to end currents in

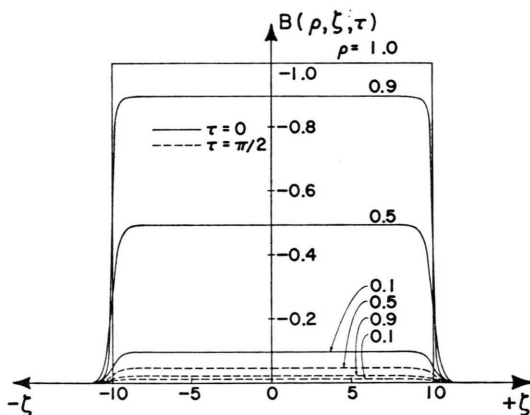


Fig. 3. Magnetic field  $B(\rho, \zeta, \tau)$  versus  $\zeta$  for  $\rho = 0.1, 0.5, 0.9, 1.0$ , and  $\tau = 0, \pi/2$ .

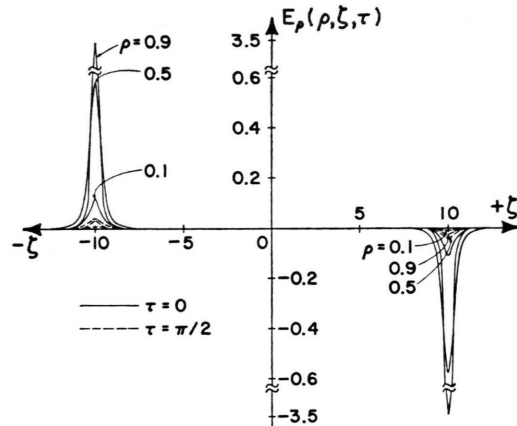


Fig. 4. Radial electric field  $E_\rho(\rho, \zeta, \tau)$  versus  $\zeta$  for  $\rho = 0.1, 0.5, 0.9$ , and  $\tau = 0, \pi/2$ .

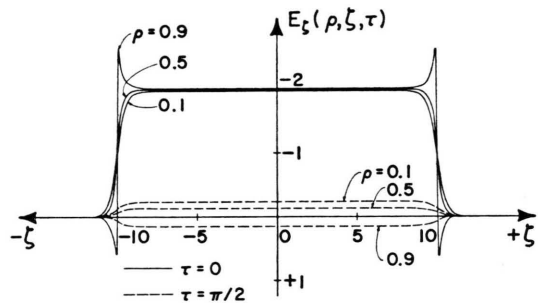


Fig. 5. Axial electric field  $E_\zeta(\rho, \zeta, \tau)$  versus  $\zeta$  for  $\rho = 0.1, 0.5, 0.9$ , and  $\tau = 0, \pi/2$ .

the region  $|\zeta| \geq \bar{c}$ ,  $\mathcal{B}(\rho, \zeta, \tau)$  exhibits end-effects in the region  $|\zeta| \geq \bar{c}$  for any  $0 < \rho < \bar{a}$ .

Figure 4 shows that  $\mathcal{E}_\rho(\rho, \zeta, \tau) \cong 0$  for  $|\zeta| < \bar{c}$  and peaks in the electrode regions  $|\zeta| \cong \bar{c}$  for any  $0 < \rho \leq \bar{a}$  [cf. Equation (39)]. For  $|\zeta| \geq \bar{c}$ ,  $\mathcal{E}_\rho(\rho, \zeta, \tau)$  exhibits end-effects which are proportional to the radial end currents.

Figure 5 shows that  $\mathcal{E}_\zeta(\rho, \zeta, \tau)$  has a plateau in the axial region  $|\zeta| < \bar{c}$  for any  $0 < \rho \leq \bar{a}$ , and exhibits end-effects for  $|\zeta| \geq \bar{c}$  which are proportional to the axial end currents. For  $\rho \rightarrow \bar{a}$  and  $\tau \neq \pi/2, 3\pi/2, \dots$ ,  $\mathcal{E}_\zeta(\rho, \zeta, \tau)$  exhibits peaks of opposite sign for  $|\zeta| \lesssim \bar{c}$  and  $|\zeta| \gtrsim \bar{c}$ , respectively [cf. Equation (40)].

### Application

For the experimental determination of the frequency dependent (spatial average) electrical conductivity  $\sigma$  of tissue, a pair of electrodes injecting the current  $I(t) = I_0 \cos \omega t$  is applied to the sur-

face  $r=a$  of the limb (with blood flow temporarily interrupted) at the axial positions  $z=\pm c$ . Another pair of potential electrodes is applied to the limb surface  $r=a$  at the axial position  $z=\pm d$ . One chooses  $d$  sufficiently smaller than  $c$  so that no perturbing edge effects from the current electrodes are picked up. These potential electrodes are connected to a (high-ohmic) ac-voltage meter, which measures the root-mean-square voltage  $\sqrt{\langle U^2(t) \rangle}$ , or to an oscilloscope which quantitatively depicts the voltage  $U(t)$ , between the sections ( $r=a$ ,  $z=\pm d$ ). In dimensionless form, this voltage is theoretically given by

$$\begin{aligned}\bar{U}(\tau) &= \Phi(+\bar{d}, \tau) - \Phi(-\bar{d}, \tau) \\ &= -\operatorname{Re} \int_{-\bar{d}}^{+\bar{d}} \mathcal{E}_z(\varrho = \bar{a}, \zeta, \tau) d\zeta\end{aligned}\quad (47)$$

i.e.,

$$\bar{U}(\tau) = \sum_{\nu=0}^{\infty} (A_{\nu} \cos \tau + B_{\nu} \sin \tau) \quad (48)$$

by Equation (40). The coefficients  $A_{\nu}$  and  $B_{\nu}$  depend on  $\sigma$  and the system parameters  $I_0$ ,  $\omega$ ,  $a$ ,  $c$ ,  $d$  [Equations (8), (12)–(13), (30)]:

$$\begin{aligned}A_0 &= \frac{|\bar{c} - \bar{d}| - |\bar{c} + \bar{d}|}{\sqrt{2} [\operatorname{ber}_1^2(\bar{a}) + \operatorname{bei}_1^2(\bar{a})]} \\ &\quad \cdot \{ [\operatorname{ber}(\bar{a}) + \operatorname{bei}(\bar{a})] \operatorname{ber}_1(\bar{a}) \\ &\quad - [\operatorname{ber}(\bar{a}) - \operatorname{bei}(\bar{a})] \operatorname{bei}_1(\bar{a}) \},\end{aligned}\quad (49)$$

$$\begin{aligned}B_0 &= \frac{|\bar{c} - \bar{d}| - |\bar{c} + \bar{d}|}{\sqrt{2} [\operatorname{ber}_1^2(\bar{a}) + \operatorname{bei}_1^2(\bar{a})]} \\ &\quad \cdot \{ [\operatorname{ber}(\bar{a}) - \operatorname{bei}(\bar{a})] \operatorname{ber}_1(\bar{a}) \\ &\quad + [\operatorname{ber}(\bar{a}) + \operatorname{bei}(\bar{a})] \operatorname{bei}_1(\bar{a}) \},\end{aligned}\quad (50)$$

and for  $\nu = 1, 2, \dots, \infty$ :

$$\begin{aligned}A_{\nu} &= \frac{2\alpha_{\nu}^2/\bar{a}}{(1 + \alpha_{\nu}^4)(p_{\nu}^2 + q_{\nu}^2)} \\ &\quad \cdot [(p_{\nu}\alpha_{\nu}^2 - q_{\nu})C_{\nu} - (q_{\nu}\alpha_{\nu}^2 + p_{\nu})S_{\nu}],\end{aligned}\quad (51)$$

$$\begin{aligned}B_{\nu} &= \frac{2\alpha_{\nu}^2/\bar{a}}{(1 + \alpha_{\nu}^4)(p_{\nu}^2 + q_{\nu}^2)} \\ &\quad \cdot [(q_{\nu}\alpha_{\nu}^2 + p_{\nu})C_{\nu} + (p_{\nu}\alpha_{\nu}^2 - q_{\nu})S_{\nu}],\end{aligned}\quad (52)$$

where

$$\begin{aligned}C_{\nu} &= \cos q_{\nu} |\bar{c} - \bar{d}| \exp\{-p_{\nu} |\bar{c} - \bar{d}|\} \\ &\quad - \cos q_{\nu} |\bar{c} + \bar{d}| \exp\{-p_{\nu} |\bar{c} + \bar{d}|\},\end{aligned}\quad (53)$$

$$\begin{aligned}S_{\nu} &= \sin q_{\nu} |\bar{c} - \bar{d}| \exp\{-p_{\nu} |\bar{c} - \bar{d}|\} \\ &\quad - \sin q_{\nu} |\bar{c} + \bar{d}| \exp\{-p_{\nu} |\bar{c} + \bar{d}|\}.\end{aligned}\quad (54)$$

The corresponding dimensional potential difference  $U(t)$  in volts is obtained in accordance with

$$U(t) = U_0 \bar{U}(\tau), \quad U_0 = \sigma^{-1} I_0 / 2\pi a. \quad (55)$$

The extrema of  $\bar{U}(\tau)$  occur at the times  $\tau = \hat{\tau}$  for which  $\bar{U}'(\tau) = 0$ . According to Eq. (48),

$$\hat{\tau} = \arctg \left( \frac{\sum_{\nu=0}^{\infty} B_{\nu} / \sum_{\nu=0}^{\infty} A_{\nu}}{\sum_{\nu=0}^{\infty} A_{\nu}} \right), \quad (56)$$

where  $\bar{U}''(\hat{\tau}) = -\bar{U}(\hat{\tau}) \gtrless 0$  for the minima ( $>$ ) and maxima ( $<$ ), respectively. Equation (43) gives for the dimensionless rms voltage

$$\begin{aligned}\sqrt{\langle \bar{U}^2(\tau) \rangle} &= \left[ \frac{1}{2\pi} \int_0^{2\pi} \bar{U}^2(\tau) d\tau \right]^{1/2} \\ &= \left[ \left( \sum_{\nu=0}^{\infty} A_{\nu} \right)^2 + \left( \sum_{\nu=0}^{\infty} B_{\nu} \right)^2 \right]^{1/2} / 2^{1/2}.\end{aligned}\quad (57)$$

It is seen that the tissue conductivity  $\sigma$  can be calculated i) by means of Eqs. (48) and (56) from the measured value of an extremum  $\bar{U}(\hat{\tau})$ , or ii) by means of Eq. (57) from the measured rms voltage  $\sqrt{\langle \bar{U}^2(\tau) \rangle}$ . These applications are complicated by the complex  $\sigma$ -dependence of the series coefficients  $A_{\nu}$  and  $B_{\nu}$  [Eqs. (49)–(54)] in which

$$\begin{aligned}\bar{a} &= a(\omega\mu\sigma)^{1/2}, \quad \bar{c} = c(\omega\mu\sigma)^{1/2}, \\ \bar{d} &= d(\omega\mu\sigma)^{1/2},\end{aligned}\quad (58)$$

$$\alpha_{\nu} = x_{\nu} / [a(\omega\mu\sigma)^{1/2}], \quad (59)$$

$$\begin{aligned}p_{\nu} &= 2^{-1/2} \{ x_{\nu}^2 + [a^4(\omega\mu\sigma)^2 + \\ &\quad + x_{\nu}^4]^{1/2} \}^{1/2} / a(\omega\mu\sigma)^{1/2}, \quad q_{\nu} = 1/2 p_{\nu}.\end{aligned}\quad (60)$$

The dimensionless numbers  $x_{\nu} \geq 0$ ,  $\nu = 1, 2, 3 \dots$  [Eq. (30)], are the roots of  $J_1(x_{\nu}) = 0$  for which an analytical representation exists [7].

Since typical values for the conductivity of biological tissues are less than  $1 \text{ mho m}^{-1}$ , we have  $\bar{a} \ll 1$  and  $\alpha_{\nu} \gg 1$  at frequencies smaller than or of the order of  $10^5 \text{ sec}^{-1}$ . In this case, Eqs. (49)–(52) indicate that

$$|A_0| \cong |-4\bar{d}/\bar{a}| \gg |B_0| \cong \bar{a}\bar{d}, \quad (61)$$

$$\begin{aligned}A_{\nu} &\cong 2[\exp\{-\alpha_{\nu} |\bar{c} - \bar{d}|\} \\ &\quad - \exp\{-\alpha_{\nu} |\bar{c} + \bar{d}|\}] / \alpha_{\nu} \bar{a} \gg B_{\nu}, \\ \nu &= 1, 2, 3 \dots,\end{aligned}\quad (62)$$

with

$$|A_0| \gg \sum_{\nu=1}^{\infty} A_{\nu}. \quad (63)$$

Hence, the root-mean-square voltage,  $\sqrt{\langle U^2(t) \rangle} = U_0 \sqrt{\langle \bar{U}^2(\tau) \rangle}$ , between the cylinder sections ( $r=a$ ,

$z = \pm d$ ) is approximately [Eqs. (55), (57) and (61)]

$$\sqrt{\langle U^2(t) \rangle} \cong U_0 |A_0| / \sqrt{2} \cong \frac{I_0}{\sqrt{2} \sigma} \frac{2d}{\pi a^2}. \quad (64)$$

This expression corresponds to the voltage between two equipotential end surfaces of a cylindrical conductor  $\sigma$ , of cross sectional area  $\pi a^2$  and length  $2d$ , carrying a homogeneous current  $I_0/\sqrt{2}$ . It should be noted that the simple result in Eq. (64) is applicable only to poor conductors such as biological tissues.

The rms voltage  $U(d) \equiv \sqrt{\langle U^2 \rangle}$  on the surface of a human thigh of average radius  $a = 0.079$  m was measured for various distances  $2d$  of the voltage electrodes and a fixed current of  $I_0 = 2.27\sqrt{2} \times 10^{-3}$  amp and frequency  $\omega = 2\pi \times 10^5$  sec $^{-1}$ . The latter was injected by means of current electrodes just above the knee and below the hip so that there separation distance was  $2c = 0.35$  m. The current and voltage electrodes were circumferential electrodes of width 0.01 m. The experimental values  $\bar{U}(d)$  and the tissue conductivities  $\sigma$  calculated by iteration of Eq. (57), with the first iteration value of  $\sigma$  determined by means of Eq. (64), are presented in Table 1.

The experimental data indicate that  $U(d)$  increases stronger than proportional to  $d$  at large distances  $2d$  and  $U(d) \propto d$  for small distances  $2d$ . For this reason, larger tissue conductivities  $\sigma$  are obtained for small values of  $d$  than for large values of  $d$ . The observed conductivities are, however, of the correct magnitude for human tissue [3, 4]. Evidently, for separation distances  $2d$  which are of the same magnitude-of-order as the width of the voltage electrodes, these perturb each other considerably so that the idealized theory which assumes circumferential electrodes of vanishing width is no longer applicable. Furthermore, for small distances  $2d$ , the thigh resembles better a cylindrical conductor of radius  $a$  than for large distances  $2d$  when the thigh resembles more a conoid cylinder. The apparent dependence of  $\sigma$  on  $d$  for fixed values of  $a$ ,  $c$ ,  $I_0$ ,

and  $\omega$  shall be studied in more detail in an experimental investigation.

### Appendix to Eqs. (31)–(33)

Equation (31) is directly obtained by integration of Eq. (24) with the help of the Cauchy integral theorem for the path of integration in Fig. 2a, since the integral along the semi-circle  $\mathcal{R}_\infty$  vanishes in the limit  $\mathcal{R}_\infty \rightarrow \infty$ . Since

$$\mathcal{E}_\varrho = -\partial \mathcal{B} / \partial \zeta \quad \text{and} \quad \mathcal{E}_\zeta = \varrho^{-1} \partial (\varrho \mathcal{B}) / \partial \varrho$$

by Eq. (7), it is simpler to derive Eqs. (32) and (33) by partial differentiation of Eq. (31) than to integrate Eqs. (25) and (26). The  $\zeta$ -derivative of the  $\text{sgn}(\bar{c} \pm \zeta)$  functions in the first expression and the  $\nu$ -sum of Eq. (31) produce terms linear in the Dirac functions  $\delta(\zeta \pm \bar{c})$ , which combine to the first expression of Equation (32). This is readily shown by means of the following theorem for Bessel functions.

In accordance with the Cauchy integral theorem, the closed integral in the complex plane  $\alpha = u + iv$  of Fig. 2a,

$$\oint \frac{I_1(\sqrt{i + \alpha^2} \varrho)}{I_1(\sqrt{i + \alpha^2} \bar{a})} \frac{d\alpha}{\alpha} \quad (A1)$$

$$= 2\pi i \sum_{\nu=1}^{\infty} \text{Res}(\alpha = i\sqrt{i + \alpha_\nu^2}), \quad 0 \leq \varrho < \bar{a},$$

can be expressed in terms of the residues of its poles at  $\alpha = i\sqrt{i + \alpha_\nu^2}$ ,  $\nu = 1, 2, \dots, \infty$ . Noting that the integral along the semi-circle  $R_0$  is  $-\pi i \text{Res}(\alpha = 0)$  in the limit  $R_0 \rightarrow 0$ , Eq. (A1) becomes

$$\int_{-\infty}^{+\infty} \frac{I_1(\sqrt{i + u^2} \varrho)}{I_1(\sqrt{i + u^2} \bar{a})} \frac{du}{u} - \pi i \text{Res}(\alpha = 0)$$

$$+ \lim_{R_\infty \rightarrow \infty} \int_{R_\infty} \frac{I_1(\sqrt{i + \alpha^2} \varrho)}{I_1(\sqrt{i + \alpha^2} \bar{a})} \frac{d\alpha}{\alpha} \quad (A2)$$

$$= 2\pi i \sum_{\nu=1}^{\infty} \text{Res}(\alpha = i\sqrt{i + \alpha_\nu^2}), \quad 0 \leq \varrho < \bar{a}.$$

The  $du$ - and  $d\alpha$ -integrals in Eq. (A2) vanish since the integrand of the former is odd in  $u$  and the integrand of the latter vanishes in the limit  $R_\infty \rightarrow \infty$ . Thus Eq. (A2) reduces to

$$\text{Res}(\alpha = 0) + 2 \sum_{\nu=1}^{\infty} \text{Res}(\alpha = i\sqrt{i + \alpha_\nu^2}) = 0,$$

$$0 \leq \varrho < \bar{a}. \quad (A3)$$

Table I.

$d$ [m]	$U(d)$ [volt]	$\sigma$ [mho/m]
0.025	0.010	0.690
0.075	0.066	0.314
0.125	0.155	0.224
0.150	0.224	0.190

Substitution of the residues of the integrand in Eq. (A1) for the indicated poles  $\alpha$  results in the fundamental equation:

$$\frac{I_1(\sqrt{i}\rho)}{I_1(\sqrt{i}\bar{a})} + \frac{2}{\bar{a}} \sum_{v=1}^{\infty} \frac{\alpha_v(\alpha_v^2 - i)}{1 + \alpha_v^4} \frac{J_1(\alpha_v \rho)}{J_0(\alpha_v \bar{a})} = 0, \quad 0 \leq \rho < \bar{a}, \quad (\text{A4})$$

$$\text{or} \quad \frac{J_1(\rho e^{i3\pi/4})}{J_1(\bar{a} e^{i3\pi/4})} = -\frac{2}{\bar{a}} \sum_{v=1}^{\infty} \frac{\alpha_v(\alpha_v^2 - i)}{1 + \alpha_v^4} \frac{J_1(\alpha_v \rho)}{J_0(\alpha_v \bar{a})}, \quad 0 \leq \rho < \bar{a}, \quad (\text{A5})$$

where  $\alpha_v \bar{a} \geq 0$  are the roots of  $J_1(\alpha_v \bar{a}) = 0$ , Equation (30). By means of Eq. (A5), Eq. (32) follows as explained above.

- [1] A. Sommerfeld, *Phys. Z.* **8**, 805 (1907).
- [2] I. N. Sneddon, *Mixed Boundary-Value Problems in Potential Theory*. North Holland Publ. Co., Amsterdam 1966.
- [3] J. Nyöber *et al.*, *J. Clin. Inves.* **19**, 963 (1940).
- [4] B. H. Brown *et al.*, *Med. Biol. Eng.* **13**, 674 (1975).
- [5] L. D. Landau and E. M. Lifshitz, *Electrodynamics of Continuous Media*, Pergamon Press, New York 1960.
- [6] F. B. Hildebrand, *Advanced Calculus*, Prentice Hall Inc., Englewood Cliff 1963, pp. 558.
- [7] E. Jahnke and F. Emde, *Tables of Functions*, Dover Publ. Inc., New York 1945.